AIAA 2001-3581
THE EFFECTS OF AL PARTICLE SIZE ON THE BURNING RATE AND RESIDUAL OXIDE IN ALUMINIZED PROPELLANTS

A. Dokhan, E. W. Price, R. K. Sigman,
and J. M. Seitzman
School of Aerospace Engineering
Georgia Institute of Technology
Atlanta, GA

37th AIAA/ASME/SAE/ASEE
Joint Propulsion Conference and Exhibit

AIAA-2001-3581

The Effects of Al Particle Size on the Burning Rate and Residual Oxide in Aluminized Propellants

A. Dokhan*, E. W. Price**, R. K. Sigman†, and J. M. Seitzman§

Georgia Institute of Technology
Propellant Combustion Laboratory
School of Aerospace Engineering
Atlanta, GA 30332-0150

Abstract

The effect was examined of aluminum particle size and of bimodal Al particle size on the burning rate of propellants and the particle size distribution of residual product Al_2O_3. It is shown that major modification of the burning rate and product size can be achieved by replacement of 20% of the conventional Al by 0.1μm Al. These effects result from the presence of an intense near surface Al flame when 0.1μm fine Al is present.

Nomenclature

D = Diameter of particles
F = Force on the particle
g = Gravitational constant
m_{res} = Expected weight of all condensed phase material.
m = Weight of the material in the sieve.
w = Weight fraction
w_{src} = Weight of the smoke condensed residue
r = Radius of particle
μ = Dynamic Viscosity of Ethanol
ρ = Density of ethanol liquid
v_∞ = Velocity of the particle

Subscripts

c = Coarse sized particles 212-106 μm
f = Fine sized particles 45-10 μm
m = Medium sized particles 106-45μm

Introduction

Aluminum(Al) powder is used as an ingredient in solid propellants to increase the propellant density and exhaust gas temperature, with a resulting increase in specific impulse of about 10%[(1)]. Compared to other metal additives, Al has the advantages of relatively low cost and good safety, and is therefore used in a wide range of tactical and large booster motors.

The primary product of Al oxidation is Al oxide (Al_2O_3), a condensed phase product. The resulting particles are responsible for undesirable side effects such as smoke exhaust trails, slag accumulation, and nozzle erosion. The oxide particles do produce an extremely desirable effect; they can provide efficient damping of combustion instability (e.g., pressure oscillations).

Al_2O_3 exhaust particle can be divided into two general size ranges: smoke oxide (diameters below ~1 μm) is formed by condensation of the gas-phase reaction products in the region surrounding a burning aluminum particle. Oxide smoke generally accounts for about 80-90% of the oxide formed by combustion and is only effective in damping high frequency oscillations, typically above 4000 Hz. Larger residual oxide particles can be formed from the oxide skin that surrounded the original Al particle, as well as additional oxide formed by condensed phase surface reactions during the course of the combustion of the particle. These residual oxide particles are effective at damping low to mid frequency oscillations. For example, the optimum particle size for damping ~500Hz oscillations is 10-30 μm[(2)].

Since the size of the residual oxide particles is related to the size of the original Al particle (in the absence of agglomeration), the choice of the Al particle size can be used to help tailor the size of the Al_2O_3 residual oxide particles. There is also some evidence that the size of the Al particles can have an influence on propellant burning rates. Specifically, the use of ultrafine Al has been suggested to produce large increases in propellant burning rates.

Therefore, the goal this research is the investigation of the influence of Al size on the burning rates and residual oxide products of aluminized propellants. High speed combustion photography, burning rate measurements, and residual oxide size distributions were obtained for a number of aluminized propellant formulations designed and manufactured at the Georgia Tech(GT) Propellant Combustion Laboratory. The

*Ph.D. Candidate. Student Member. Email:allandokhan@hotmail.com
**Regent's Professor Emeritus, Fellow AIAA
†Senior Research Engineer/ Emeritus
§Associate Professor, Senior Member AIAA

propellants were based on bimodal ammonium perchlorate (AP) and Al distributions.

Background

For conventional-sized Al, the Al in a AP-binder propellant is initially clustered due to packing patterns in the presence of much larger AP particles. The Al particles sit in a matrix of binder and fine AP particles. The binder/AP/Al matrix is very fuel rich. When a submerged Al particle is exposed to the burning surface, it is usually stuck in a layer of semi-liquid binder. Since Al does not evaporate or decompose like other ingredients; it has been observed that the Al tends to reside on the surface. This leads to concentrations and interactions of particles, to a degree that is dependent (among other things) on the degree of clustering originally present in the propellant's microstructure.

While Al is extremely reactive, the particles have a refractory coating of Al_2O_3 (the oxide skin) that minimizes further contact of Al and oxidizer molecules until temperatures are high enough to degrade the protectiveness of the oxide coating. The surface concentration sets the stage for interparticle sintering, while the protective oxide limits the degree of oxidation. Concentration and sintering continues until the assemblages detach from the surface or inflame on the surface. In either case, the temperatures quickly becomes so high that the sintered assemblages melt down into droplets, commonly referred to as agglomerates, which burn in the hot gas flow above the propellant surface [(1)].

The details of this concentration-sintering-detachment-agglomeration process are important because they affect the site and extent of the Al combustion and the size of the product oxide droplets. These in turn impact propellant burning rates, combustion efficiency, combustion stability, and slag formation. Of the many propellant formulation variables that affect the Al behavior, the present study selects a restricted set aimed at the control and verification of the behavior. PBAN-ECA-DOA binder at the 11% level was chosen because it is widely used. Al at the 18% level was chosen for the same reason. A bimodal AP size distribution was chosen because, (a) earlier research studies[(3)] had used bimodal AP (with 10μm and 82.5μm fine particle size), (b) bimodal leads to easily understood and controlled packing patterns and combustion zone structure, and (c) bimodal can lead to desirable plateau burning.

The formulations of GT's propellants are founded upon the desire of tailoring formulations to specific applicational needs. The use of ultra-fine Al with conventional sized Al is selected to give optimum residual size for damping unstable combustion, or with relative amounts selected to tailoring burning rates.

The difficulties in tailoring the residual oxide size have been reported in previous papers[(4)]. Uncertainties based on the size of the burning droplet leaving the surface due to surface agglomeration; burning histories of single particles vs. agglomerates; and the final burnout phase (where fragmentation and ejection of droplets have been viewed in laboratory experiments) introduce complications beyond the scope of even the most advanced single particle burning theories. Modifications to the ingredient powder to reduce or eliminate surface agglomeration and thus promote single particle combustion[(5, 6)] would remove the ambiguity of the initial ignited particle size and composition. The experimental results and analytical approaches developed should be applicable to actual propellant problems. While such modifications may increase the cost of ingredients, they may decrease the overall program costs.

Experimental Methods

Propellant Formulations

This study is focused on the behavior of Al in the propellant combustion zone. The Al particle size is a primary variable. However, Al behavior is also known to depend on other formulation variables. The choice of values of other variables were based on two criteria: (a) Consistency with current practical standards "in the trade", and (b) ideas on how to tailor the Al behavior. Under criterion (a) all formulations had 89% solids, 11% PBAN binder, 18% Al, and 71% AP oxidizer. Under criterion (b) bimodal size distribution were used for AP and for Al. In all formulations the coarse AP particle size was 400μm (nominal) and the fine AP particle size was either 82.5 or 10μm (nominal). The mass ratio of the coarse AP to fine AP (AP c/f) was a primary variable. In most formulations the coarse Al particle size was 30μm (nominal) and the fine Al particle size was 0.1μm (nominal). The mass ratio of the coarse to fine Al (Al c/f) was a primary variable. The fine AP size was also a primary variable to the extent of a choice between 82.5μm and 10μm. There was one exception to the above, i.e. series of formulations involved variation of the coarse Al size from 30 to 0.1μm (with unimodal distribution). A list of the formulations is contained in Table 1, Table 2 and Table 3. Use of bimodal Al particle size distribution was motivated by the idea that the ultra fine Al would enhance the burning rate and reduce the degree of agglomeration of the Al, while the particle size of the coarse Al would influence the size of the product oxide (Al_2O_3) droplets.

The ingredients were chosen from supplies readily available. The 400μm coarse AP was chosen because it provided latitude for wide range of choice of the particle size of the fine AP. In addition, the combination of the 400 and 82.5μm AP had been used in an earlier study[3] that provided valuable insight into Al behavior. The 400μm AP was supplied by WECCO. The 82.5μm AP was prepared from WECCO 200μm AP. The 10μm AP was supplied by Dr. Karl Kraeutle (US Naval Warfare Center, China Lake). All AP was relatively high purity with no anti-coating agent. Four Al particles size were used. The "H" series(H-30, H-15, H-3) were supplied by Valley Metalurgical Company (Valimet) and are nominally 30, 15 and 3 μm. The fourth size is ultrafine (nominal 0.1 μm) with the trade name "Alex" supplied by Argonide.

PBAN-Prepolymer	Epoxy Curing Agnet	DOA-Plasticizer
63.18%	21.04%	15.78%

Table 1: Binder formulation based upon mass percentage.

Binder	AP	Al
11%	71%	18%

Table 2: Propellant formulations based upon mass percentage.

Mix #	APf	Alc	Alf	AP c/f	Al c/f
1B	82.5	H-15	0	80/20	100/0
2	82.5	H-30	0	80/20	100/0
4	82.5	H-3	0	80/20	100/0
5	82.5	Alex	0	80/20	0/100
6	82.5	H-30	Alex	80/20	50/50
7	10	H-30	Alex	70/30	50/50
8	10	H-30	Alex	60/40	50/50
9	82.5	H-30	Alex	80/20	80/20
11	10	H-30	0	80/20	100/0
12	10	H-30	Alex	80/20	50/50
13	10	H-30	Alex	80/20	50/50
14	10	H-30	Alex	50//50	50/50
15	82.5	H-30	Alex	60/40	50/50

Table 3: Propellant variables.

In house propellants where manufactured using an in house designed small scale solid propellant mixer[7]. Propellants were mixed by adding binder first, composed of the polymer, plasticizer (DOA) and curative agent (ECA). The addition of fine AP, followed by the course AP and then the Al were then added. Each time a new ingredient was added to the mix, it was stirred for approximately 20 minutes to allow appropriate distribution of the ingredients. The propellant is placed in the propellant mixer where it was allowed to mix for approximately 1 hour.

Techniques

Experimental techniques used in this study. (1) Combustion photography/burning rate, and (2) Particle collection bomb.

1. Combustion photography was used in obtaining the burning rates of propellants. A high-speed digital imaging(RL) camera operated at 1000 frames per second with an exposure time of approximately 67μs was used to measure the regression of the burning surface frame by frame.

The propellant sample is cut approximately to 4x3.5x10 (mm) where it is glued to a support using epoxy glue. A finely coiled nichrome wire (covering larger surface area) is then firmly placed over the top-end of the propellant at which then the unit (holding the propellant) is attached into the lower end of the combustion bomb.

2. The collection vessel used consists of a stainless steel pressurized collection vessel (length = 67.31cm [26.5 in], internal diameter =5.08cm [2 in], volume = 1524 cm^3 [93 in^3]), which is connected to a large surge tank (volume = 49830 cm^3 [3041 in^3]). A porous sintered stainless steel plate separates the two vessels to provide some filtration of the gas expansion into the surge tank during combustion. The collection vessel and surge tank are designed for pressures of over 206.8 bars (3000 psi). The collection vessel is modular and can be extended by adding stainless steel extensions. The standard three extension vessel is 34.92 cm (13.75 in) in length (volume = 721 cm^3 [44 in^3]) for a 20.32 cm (8 in) plume tube, allows for 6.98cm (2.75 in) for mounting fixture and ethanol bath, while the five extension set up is 50.17 cm (19.75 in) in length (plume tube: 43.18 cm [17 in], volume = 1016 cm^3 [62 in^3]), and the 7 extension set up is 65.41 cm (25.75 in) in length (plume tube: 58.42 cm [23 in], volume = 1344 cm^3 [82 in^3]). With an approximately 7-gram propellant sample, a pressure rise of typically 0.7-2 MPa (100-300 psi) from a static test at 6.9 MPa (1000psi) was observed but this is dependent upon propellants used and mass addition from burning propellants. See Figure 1.

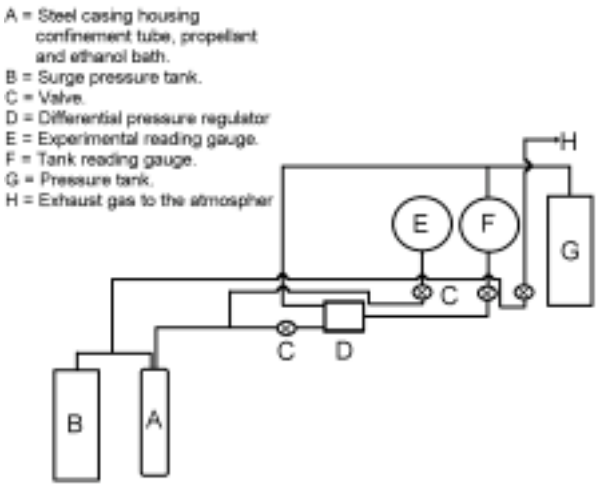

(a)

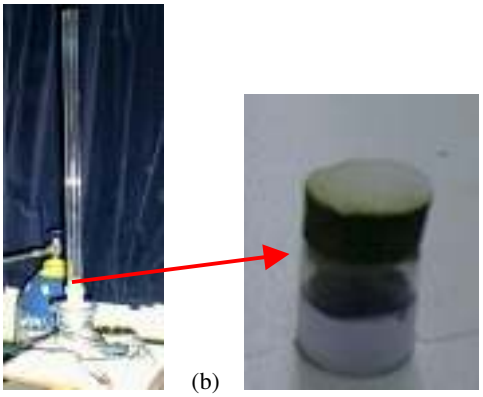

(b) (c)

Figure 1: (a) Experimental arrangement of particle collection bomb, (b) Quartz plume tube without the Al-foil placed in the steel housing case "diagram (a)" inverted, (c) Propellant attached to the propellant holder and with AP-igniter paste spread on the top of the solid fuel.

The material for the plume tube was difficult. Previous tests with a thin walled stainless steel tube indicated a rapid temperature drop off[8] and the confinement tubes were replaced with quartz. Quartz is preferable to stainless steel for the plume confinement tube due to its lower thermal conductivity. Problems with the quartz plume tube cracking and contaminating the residue are overcome by the use of a hollow quartz plug (same thermal expansion coefficient as the quartz material for the confinement tube) with O-rings used as support between the confinement tube and the nylon pins holding the plume tube in place. This allows for differential expansion of all components. When carefully assembled, this procedure does not result in any cracking of the tube. All tests were and are ran with a quartz plume tube with a 2.54 cm (1 in) diameter, 0.15 cm (0.06 in) wall thickness, and a length of 58.42 cm (23 in). Wrapping the exterior of the tube with aluminum foil also reduces heat loss from the combustion gases due to radiation [9].

The procedure is to prepare a small disk of the propellant (2.54 cm [1 in], 1cm [1/4 in] thick). The sample is sealed in a thin walled plume tube so that the Al burns in the gaseous combustion products of the propellant. The plume tube is inverted and after a long path through the plume tube, the plume impinges on a pool of anhydrous ethanol that is used as a collection medium. The experiment is conducted in a long, thick-walled pressure vessel, with the ethanol at the bottom. Following the firing, the pressure is slowly released and the pressure vessel is disassembled. The ethanol containing the residue is poured into a beaker and the residue on the plume tube and the pressure vessel are washed with a stream of ethanol and retained. The smoke combustion residue (SCR) is removed by repeated timed sedimentation and weighed. The sedimentation time is determined based upon Stokes diameter and is computed from *Stokes' law*.

$$F = \left(\frac{4}{3}.\Pi.r^3\rho.g\right)_{BuoyantForce} + \left(6.\Pi.\mu..r.v_\infty\right)_{formdrag+frictiondrag} \quad (1)$$

Using the above equation, sedimentation times can be established for specific particle diameter as shown in Figure 2.

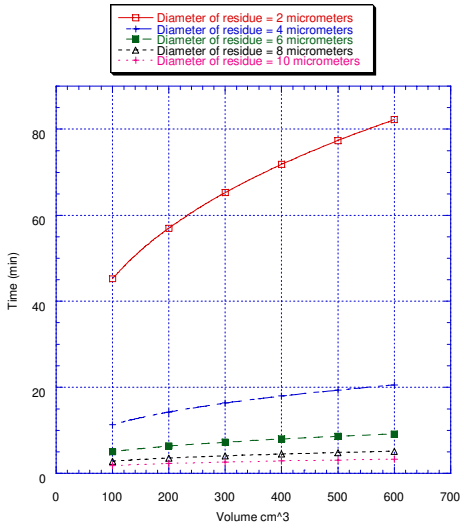

Figure 2: Sedimentation time for spherical Al_2O_3 in ethanol at given volumes.

Both the SCR and non-smoke combustion residue (NSCR) are desiccated by placing them in a fume hood and allowed to sit there for several hours. The weights of both SCR and NSCR are then recorded.

The NSCR are separated, size graded with sieves. The sieves are subdivided into 5 sub grades; D>212μm, 106μm<D<212μm, 45μm<D<106μm and 10μm<D<45μm.

The NSCR are dispersed homogeneously i.e. no particles are in contact with one another, across a microscope slide that is then mounted on a computer controlled optical microscope. The 'Leitzman Wetzlar Microscope' is made up of a Panasonic VW3260 Video cam that is used by the computer to take images of the sample, a 'fiber-lite high intensity illuminator' is used to throw light in a downwards direction on to the sample and a built in 'Leitzman Wetzlar Microscope' illuminator throws light from beneath the sample. The 3D movement of the microscope stage is controlled through the computer and manually adjusted through the application of a joystick.

A program was written and executed to digitally take pictures of the particles frame by frame and to compute and save the average diameter of these particles. This method is repeated for each sub grades i.e. 106μm<D<212μm, 45μm<D<106μm and 10μm<D<45μm. A FORTRAN program was then written to take the stored information and perform relevant combustion instability calculations, i.e. total number of particles accounted for over all sub-sieve grades, sub-sieving the particles into diameter (μm) bin sizes, mass, number density, distributions, damping frequencies, etc.

Depending upon the sub grade sieve in question, the number of particles that are counted ranges from 1000-1500 particles for a sieve range of 106μm<D<212μm to 20000-40000 particles for a sieve range of 10μm<D<45μm.

Expected Residue

The expected residue is used for the calculation of the weight fraction and because: a) the collection apparatus was not designed to collect smoke, and b) calculations of combustion stability are based on expected residue weight. The weight of the SCR , w_{scr}, is taken to be the weight of the expected residue minus the weight of the NSCR. The expected oxide is calculated from the weight of the sample, percent of Al in the sample, and the ratio of molecular weights of Al_2O_3 to Al_2.The expected residue, M_{res}, is then the sum of the expected oxide. The collection efficiency is then the ratio of the collected residue to the expected residue. Since this is a filtered-open system, the overall collection efficiency is expected to be much less than that of a closed system.

The weight from each of the sieves gives the weight fractions. The coarse sieve weight fraction is thus:

$$W_c = \frac{M_c}{M_{res}} \tag{2}$$

Where the denominator is the expected weight of all of the condensed phase material and M_c is the weight of the materiel in the coarse sieve.

Mass Distribution

Software developed in-house sorts the particles into bins based on a 10-20 micron spread in diameter (wider bins at larger diameters). The contents of each bin are computed by the equation:

$$h_{ik} = \frac{\sum_{j}^{NI} N_j D_j^3}{\sum_{j}^{NS} N_j D_j^3} \tag{3}$$

Where the upper summation (and subscript i) produces the volume in bin "I" for a given slide "k" and the lower summation gives the total volume of the particles on the slide. It is assumed that the sample actually scanned is representative of the sample in the sieve and that the density is uniform so that equation 3 also represents the mass in a bin (i) (from a sieve) divided by the total mass in the sieve (k). Since the sieving is not precise (there are a small number of fines in the mid and coarse sieves) the h is summed over the 3 sieves to give the distribution function (at the diameter at the midpoint of bin i):

$$f_i = \frac{h_{if} w_f + h_{im} w_m + h_{ic} w_c}{\Delta d} \tag{4}$$

Where Δd is the bin width (10 or 20 microns). Note that the integral (it is a piecewise continuous function) of f with respect to the diameter from 0 to 212 microns is 1.

Mass Average Diameter D_{43}

The developed software also computes the sums:

$N_i D_i^4$ and $N_i D_i^3$ for each particle on a slide to give a function d_k given by;

$$d_k = \frac{N_i D_i^4}{N_i D_i^3}$$

Where the subscript k denotes sieve: coarse, medium, fine or smoke oxide. D_{43} is then:

$$D_{43} = w_c d_c + w_m d_m + w_f d_f \qquad (4)$$

Size analysis of the SCR requires additional expensive equipment and/or development of new separation and dispersion techniques. Although great care was taken to collect as much of the smoke as possible to determine the collection efficiency, the smoke was allowed to dry into a compact mass for weighing.

Results And Discussion

As indicate above, a combination of high-speed combustion photography and residual particle collection/sampling was used to characterize the burning propellants, burning rates and measure the residual oxide size distribution. The results are represented below for propellant variations described above at pressures from 1.4-6.9MPa (200-1000psi). This paper is reporting preliminary findings.

Aluminized Burning Region (ABR)

Combustion photography showed the difference between the ABR with ultra-fine Al and conventional sized Al at the propellant surface. Figure 3, shows that the ABR for Al particle sizes 0.1μm, 3μm at 6.89MPa occurs very close to the propellant surface compared to 30μm Al. Surprisingly, results showed similar ABR for propellants with 0.1μm and 3μm Al particles. The proximity of the ABR to the propellant's surface would allow for greater heat feed back to the flame front for higher burn rates.

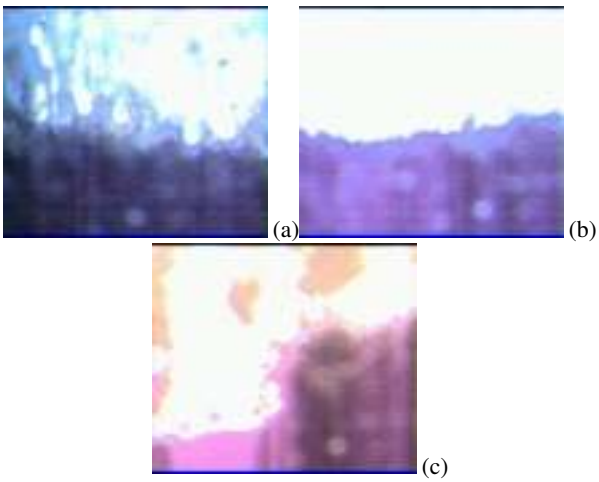

Figure 3: Aluminized burning region at 6.89MPa (1000psi) with AP-80/20(82.5) with 100%, (a) H-30, (b) H-3, (c) Ultra fine Al (~0.1μm)

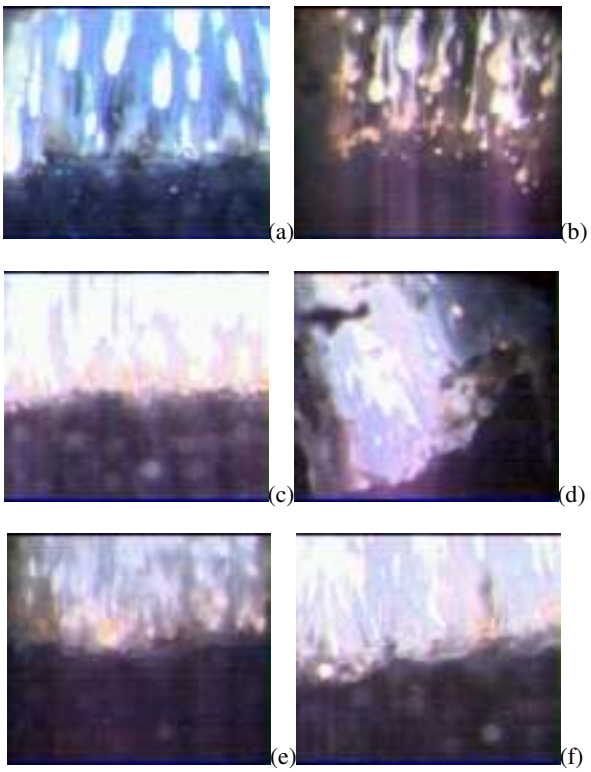

Figure 4: Images from combustion photography at 1.38MPa (200psi) for AP c/f 80/20 for bimodal Al (a) AP=10μm/100(H-30), (b) AP=82.5μm/100(H-30), (c) AP=10μm/80(H-30)-20(Alex), (d) AP=82.5μm/80(H-30)-20(Alex), (e) AP=10μm/50(H-30)-50(Alex), (f) AP=82.5μm /50(H-30)-50(Alex).

Figure 4, shows the variation in the ABR from the propellant surface for bimodal Al distribution at 1.38MPa for different fine AP. Combustion photogra-

phy shows agglomerates leaving the surface with bimodal Al propellants.

Effects of Al Particle Size on Burning Rate (Unimodal).

Measurements of the burning rate were made on four formulations with 82.5μm fine AP, and one with 10μm fine AP, with unimodal Al of 4 particle sizes. The results are shown in Figure 5.

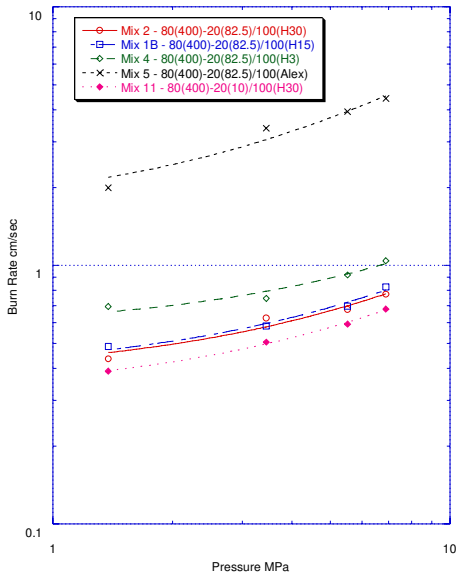

Figure 5: Burning rate verses pressure for different Al particle sizes.

The burning rates with 30μm and 15μm Al are nearly the same. The burning rate with 3μm Al is appreciably higher, and the rate with 0.1μm Al is several times that with 30μm Al. Replacement of the 82.5μm AP in the 30μm Al mix by 10μm AP led to a decrease in the burning rate.

There are noticeable differences when the Al particles are reduced by a factor of 10 (H3) and considerably when reduced by a factor of 300 (using Alex) relative to H-30. The relative increase in burning rates with H-3 was surprising and by reducing the particle size by a factor of 30 (relative to H3) does produce even larger increases in the burning rate. Figure 6 indicates the behavior that ultra fine Al exhibited in propellants are part of the continuum of what happens when reducing the size of the Al particles.

In the past, forecasting the effects of Al particle size on the propellant burning rate has been difficult because the effect depends on the complicated surface concentration-sintering-agglomeration process, which itself depends on other formulation variables. The present results indicate that very fine Al enhanced near surface heat release. The combustion photography showed intense luminosity in the region immediately above the burning surface when 0.1μm Al was used, indicating rapid Al combustion there. It was speculated that there might be some Al oxidation on the surface as well (see later). The effects of changing the fine AP size to 10μm suggest that heat release from surface reaction is not important, since the enhanced availability of oxidizer species is accompanied by a decrease in rate (30μm Al). It seems likely that the AP particle size effect is related to changes in the AP/binder flame structure.

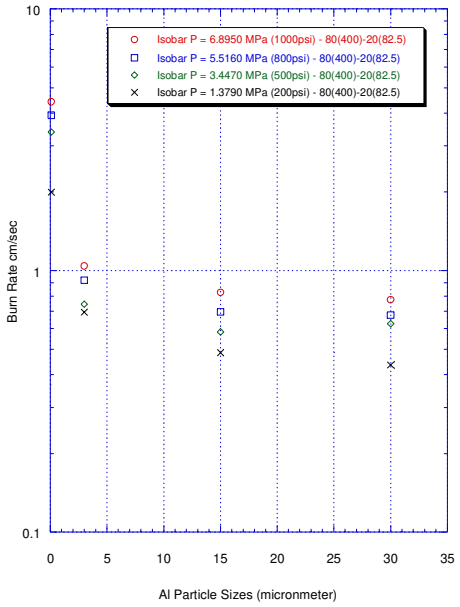

Figure 6: Burning rate verses Al particle size

Propellants with all 0.1μm Al and fine AP=10μm was found to possess poor mechanical characteristics i.e. crumbled when cut. Due to packing, it is speculated that the high fine loading contents (with 10μm AP and 0.1μm Al) prevents the binder from wetting all the particles and therefore results in poor mechanical propellants.

Effects of Al Coarse-to-Fine Ratio On Burning Rate (30μm and 0.1μm Al)

Figure 7 and Figure 8 show burning rates for formulations with bimodal Al. Figure 7(a) and Figure 8(a) are for formulations with 10μm fine AP and Figure 7(b) and Figure 8(b) are for formulations with 82.5μm fine

AP. In general, increasing the proportion of fine Al increases the burning rates. Rates with 82.5µm AP are higher than rates with 10µm AP, supporting the earlier argument that the rate enhancement with 0.1µm Al is not due to heat from oxidation of Al on the burning surface.

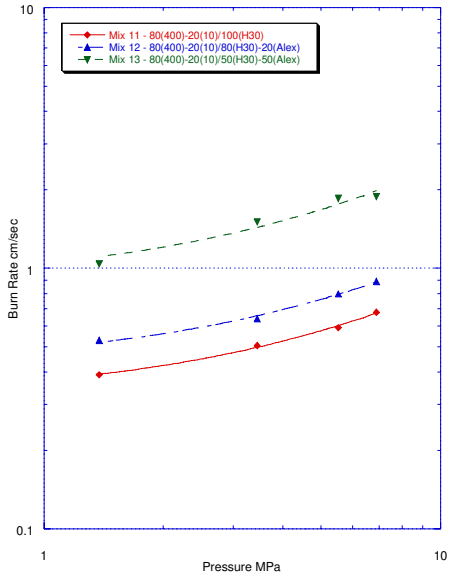

(a)

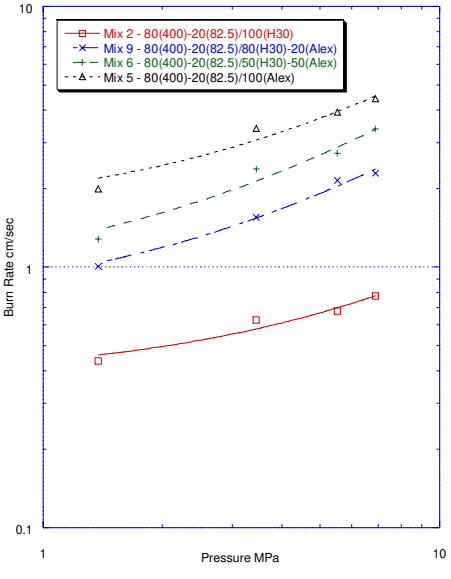

(b)

Figure 7: Burning rate vs. pressure at different aluminum coarse to fine ratio at; (a) AP = 10µm, (b) AP = 82.5µm

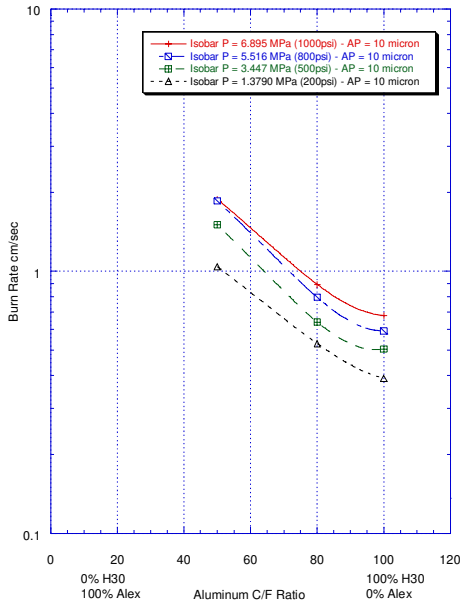

(a)

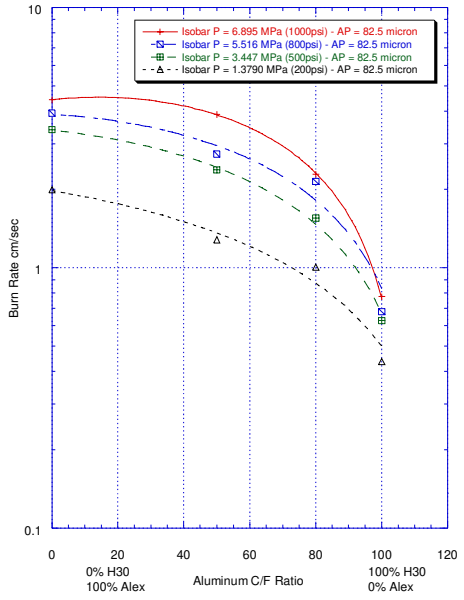

(b)

Figure 8: Burning rate vs. Al c/f ratio at different pressures for (a) AP = 10µm, (b) AP = 82.5µm.

While the intensity and location of the bright near surface flames were not quantified, these properties were qualitatively consistent with the argument that such flames contribute to burning rates (and the extraordinary brightness establishes that near surface Al combustion is involved).

From a practical viewpoint it is notable that this increase in rate was largest for the first 20% replacement of 30µm by 0.1µm Al. To achieve the "0.1µm Al effect" does not require substantial amounts to start with, (Figure 8(b)). This is referred to as a "practical view-

point" because: (a) the fine Al is expensive, (b) propellant processing is more difficult with more 0.1µm Al affecting the mechanical properties, and (c) the 0.1µm Al has a higher content of unwanted Al_2O_3. It is also notable that this "first 20%" rule was for formulations with 82.5µm fine AP, and is not applicable to the formulations with 10µm AP. Figure 8(a) and (b) indicates a relationship with Al c/f ratios that is unique to the size of the fine AP. Figure 8(b), shows the addition of small quantities of 0.1µm does produce higher burn rates and that additional 0.1µm Al above 50% does not substantially alter the burning rate of the propellants compared to increases of 100%. Figure 8(a) indicates an opposite relationship, the addition of 0.1µm Al will continue to increase the burning rate substantially, hence the steep gradients. Nonetheless this envelope is restricted due to argument (b) above.

Returning to the mechanistic arguments, the bright near-surface flames seen where fine Al is used are indication of enhanced Al burning. This suggests that ignition of Al particles is a burning-rate-controlling step. It has been argued in the past[3] that ignition occurs when the Al is hot enough for the protective oxide coating to be broken down, and that this requires proximity to near-surface hot AP/binder flamelets called "LEF-Leading Edge Flames". Earlier research indicated that fine AP particles (e.g. 10µm) burn with a cooler premixed flame[10], less conducive to ignition of Al near the surface. This may explain why the rate enhancement with 0.1µm Al is greater with 82.5µm fine AP than with 10µm fine AP.

Effects of AP Coarse-to-Fine Ratio on burning Rate.

Figure 9 shows the burning rates for formulations with 50/50 coarse to fine Al and various ratios of coarse to fine AP. Figure 9(a) is for 10µm fine AP and Figure 9(b) is for 82.5µm fine AP. As noted earlier, the burning rates for AP c/f = 80/20 were higher with 82.5µm fine AP than with 10µm fine AP. Increasing the proportion of fine AP didn't affect rate much with 82.5µm fine AP, but resulted in a large increase in rate with 10µm fine AP, to the extent that rates with 10µm fine AP were nearly the same with both fine AP sizes.

While a complete explanation of the results in Figure 9 will probably require more study, the most important message is that trends of results (as in Figure 7 and Figure 9) depend on choice of AP c/f ratio (as well as the other formulation variables that were held constant in this study). A first step in understanding the AP c/f effort is to note that the Al is contained in a very fine fuel-rich "matrix" portion of the volumes consisting of a mixture of Al, fine AP and binder.

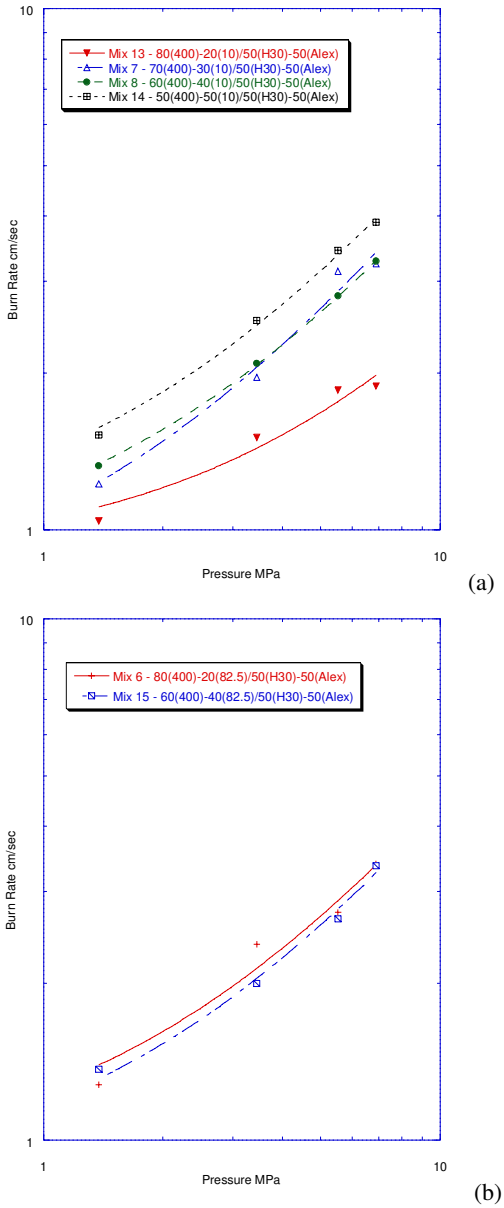

Figure 9: Burning rate vs. pressure for different AP c/f ratios for (a) AP = 10µm, (b) AP = 82.5µm.

When an Al particle is reached by the burning surface, it is initially exposed to an environment dominated by the Al-fine-AP-binder matrix. The 82.5µm fine AP is large enough to burn with hot leading edge flamelets to ignite the Al, while a matrix with 10µm fine AP either doesn't burn on its own, or burns with a relatively cool premixed flame (not conducive to igni-

tion of Al). The results in Figure 9 suggest that at higher fine AP content, the premixed flame with 10µm AP becomes competitive with LEF's as a heat source for Al ignition (and a better source for oxidizer vapors).

Size Distribution of the Residual Oxide

Combustion photography showed burning Al particles/agglomerates leaving the propellant surface at 1.38MPa, Figure 4. Figure 10 shows the mass distribution for NSCR collected for formulations that have unimodal and bimodal Al (30µm and 0.1µm Al) for AP c/f = 80/20 at 1.38MPa. Figure 10(a) is for 10µm fine AP and Figure 10(b) is for 82.5µm fine AP. Table 4 shows the computed D_{43} according only to the collected NSCR, equation (4), and NSCR mass fraction i.e. NSCR/expected residue.

The results show the collected NSCR for unimodal Al distribution with 10µm fine AP is similar to 82.5µm fine AP. Some of the NSCR seem to be left from the burn-out of single 30µm Al particle. The amounts of these particles were approximately the same for both AP sizes. There is an additional part of the NSCR that would seem to have resulted from the burn out of agglomerates. There distribution were about the same for both fine AP sizes, but the amount was twice as much for mixes with 10µm AP. Interesting enough, there is not as much of the coarse fraction of the NSCR with 82.5µm as there is with 10µm. This amounts to an observation of less total NSCR. No explanation of this has been advanced as of yet. Examination of the NSCR from Table 4, it may be noted that this "missing" NSCR is an even bigger problem as one goes to the bimodal Al distribution with 50% increases with 0.1µm Al, resulting in a reduction of NSCR by 85% to 90%, Figure 10(a) and (b). If it were assumed that the 0.1µm Al burns to SCR, this would explain the 50% reduction in NSCR leaving unexplained another 35% to 40%. The difference may be explained by the modification of the 30µm Al burning in the presence of the 0.1µm Al flame.

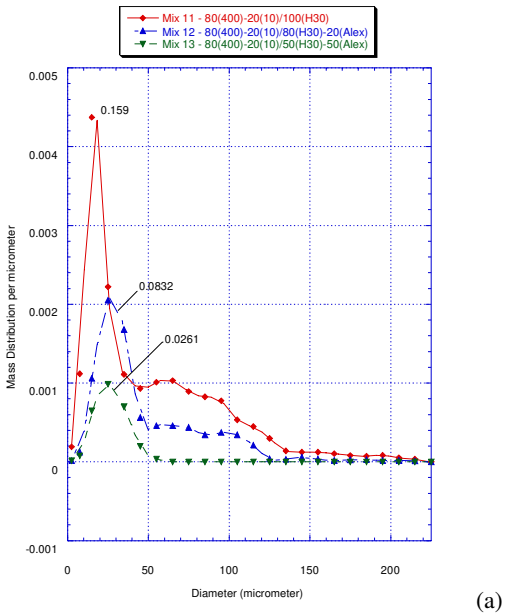

(a)

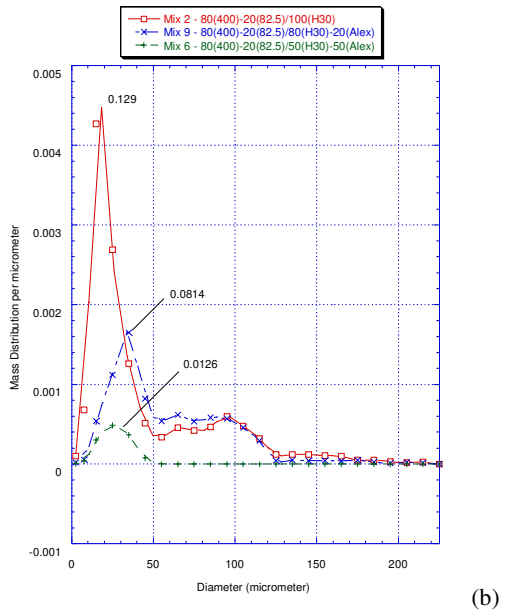

(b)

Figure 10: Mass fraction distribution vs. diameter for

(a) AP=10µm, (b) AP=82.5µm. Mass fraction of the NSCR to the total expected mass is also shown for each distribution on the graph.

Al Distribution %	AP Distribution 80(400)-20(10)	AP Distribution 80(400)-20(82.5)
0(Alex) - 100(H30)	53.28, 0.159	45.87, 0.129
20(Alex) - 80(H30)	51.38, 0.0832	61.04, 0.0814
50(Alex) - 50(H30)	26.96, 0.0261	26.33, 0.0126
100(Alex) - 0(H30)	N/A	N/A

Table 4: D43 (µm) and NSCR mass fraction for various bimodal aluminum distributions for given AP distributions.

Increases of 0.1μm Al to 50% produces the unexpected results of clumps in the sieve range of 212-106 and 106-45μm, that resembles similar results shown in Figure 11, that have not been included in the calculations of the mass distribution for mix 6 and 13. The color of these collected clumps are (dull) white and represents approximately 68% and 75% of the collected NSCR (10<D<212) for 10μm and 82.5μm fine AP respectively.

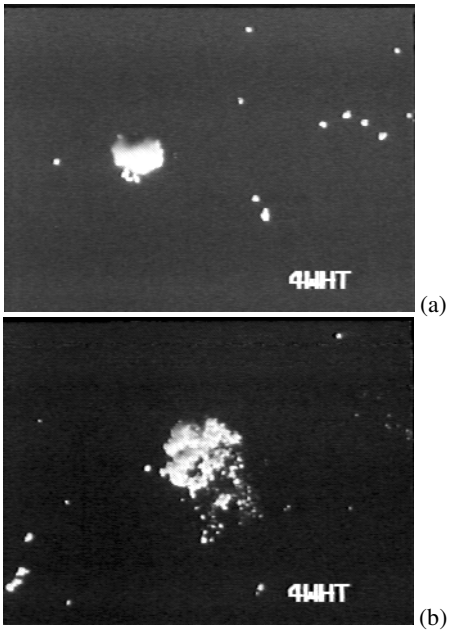

(a)

(b)

Figure 11: Images of the collected residue in sieve range 212-106, at 10x1 magnification for mix 5, (a) Collected residue resembling 'Clumps', (b) A clumped particle when tapped with a sharp pointer.

Examination of 0.1μm Al under an optical microscope showed similar clumped shaped particles, that were dark gray in color, Figure 12. Earlier research showed hotstage results indicating[11] unusual dendritic formation that resembles similar results/shapes. Therefore, it is probable that the 0.1μm Al is originally clumped in the propellant and the collected NSCR clumps are the products of the combustion of 0.1μm Al.

It is worth noting that particle collection tests were also conducted for Mix 5-80(400)-20(82.5)/100(Alex) at 1.38 bars. Residuals were collected in the sieve range of 212-106μm, 106-45μm and 45-10μm. 50%, 43% and 7% of the collected residue were in the sieve range of 212-106, 106-45 and 45-10 respectively. Closer examination of the collected residue indicated that the collected particles also resembled clumps of irregular non-spherical particles that 'crumbled' very easily when tapped with a sharp pointer, Figure 11.

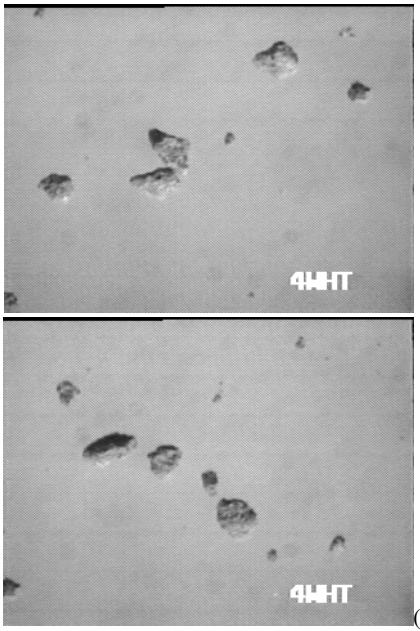

(a)

(b)

Figure 12: Images of ultra-fine Al particles at 5x1 magnification.

Summary

The combustion of propellants with bimodal Al particle size was evaluated in the range of 1.4-6.9MPa (200-1000psi) with high-speed digital photography and by collection of condensed combustion products. The photography was used to determine burning rate and metal combustion field (near surface), and the collected combustion products were used to determine the nature of the particles, and to determine the amount and size distributions of the particles in the 4 - 200μm size ranges. The propellants all used 11%PBAN binder, 18% Al and 71% bimodal AP with 400μm coarse AP and either 82.5μm or 10μm fine AP, with various ratios of coarse-to-fine.

One series of formulations had unimodal Al (30, 15, 3 and 0.1μm), with 82.5μm fine AP and AP c/f=80/20. A single comparison formulation was made with 30μm Al and 10μm fine AP. Tests on this set of propellants indicates that intense Al combustion close to the burning surfaces increases the burning rate by a factor of approximately 6 when 0.1μm Al is used in place of 30μm Al. A similar, but very modest effect was observed with 3μm Al. Comparison of the two similar mixes with different fine AP size (30μm Al) showed somewhat higher rates with 82.5μm AP-f than with 10μm AP-f. Collected oxide gave less large product particles (40-110μm range) with 82.5μm AP, indicating less Al agglomeration (or more fragmentation).

A second series of formulations had bimodal Al (30μm and 0.1μm) with different Al c/f ratios, using AP c/f ratios of 80/20 and AP-f 82.5μm or 10μm. Tests showed progressively higher burning rates as the 0.1μm Al content was increased. This trend was accompanied with an increasingly uniform and intense near surface Al flame. With 82.5μm AP-f the sensitivity of rate to increase in 0.1μm Al was high at low 0.1μm Al content (high Al c/f); sensitivity to incremental increases at higher 0.1μm Al contents was low (an important practical point because there are some problems with the use of high content of 0.1μm Al). Rates with AP-f =10μm were somewhat lower and did not show the same desirable large increases in rates with 0.1μm Al addition at low 0.1μm Al-f contents. These trends led to the conclusion that rate enhancement with 0.1μm Al is not due primarily to Al oxidation on the burning surface.

A third set of formulations had 30μm and 0.1μm Al in a 50/50 ratio, with various ratios of 400μm and 10μm AP. A limited comparison set had 82.5μm fine AP. Increasing the amount of 10μm AP increased the burning rate, probably due to increases in the temperature of the "matrix" flamelets over the fine AP-Al-binder areas of the surface (thereby improving the thermal environment for Al ignition). The two formulations with 82.5μm AP did not show this sensitivity to fine AP content, presumably because the Al ignition is controlled by hot O/F leading edge flames on each 82.5μm and 400μm AP particle[3].

Acknowledgment

The authors would like to acknowledge the Office of Naval Research (Dr. J. Goldwasser) for support in development of the particle collection - measurement facility.

References

[1] Price, E. W., and Sigman, R. K., “Combustion of Aluminized Propellants,” Solid Propellant Chemistry, Combustion, and Motor Interior Ballistics, Vol. 185 of AIAA Progress series, 2000, pp.663-687.

[2] Culick, F. E. C., “ Combustion Instabilities: Mating Dance of Chemical, Combustion, and Combustor Dynamics,” AIAA Paper 2000-3178, 36th AIAA/ASME/SAE/ASEE Joint Propulsion Conference and Exhibit, Huntsville, AL, July 16-19, 2000.

[3] Sambamurthi, J. K., and E. W. Price, “Aluminum Agglomeration in Solid Propellant Combustion”, AIAA Journal, Vol.22, August 1984, pp. 1132-1138.

[4] Sigman, R. K., Lillard, R. P., Price, E. W., Seitzman, J. M., and Dokhan, A, “Size Distribution of Resiudal Oxide Droplets from MURI Propellants,” Proceddings of the 36th JANNAF Combustion Meeting, Chemical Propulsion Information Agency, Laurel, MD, CPIA Pub. 231, Nov. 1999.

[5] Boggs, T. L., Kraeutle, K. L., and Zurn, D. E., “The Combustion of As Received and Preoxidized Aluminum in Sandwich and Propellant Configurations,” Proceedings of the 9th JANNAF Combustion Meeting, Vol. I, Chemcial Propulsion Information Agency, Laurel, MD, CPIA Pub. 231, Dec. 1972.

[6] Breiter, A. L., Mal’tsev, V. M., and Popov, E. I., “Means of Modifying Metallic Fuel in Condensed Systems,” translated from Fizika Goreniya I Vzryva, Vol. 26, No. 1, January-February 1990. pp. 97-104.

[7] Sigman, R. K., Jeenu, R., and Price, E. W., “A Small Scale Solid Propellant Mixer and Vacuum Degasser”, Proceddings of the 36th JANNAF Combustion Meeting, Chemical Propulsion Information Agency, Laurel, MD, CPIA Pub. 231, Nov. 1999

[8] E.W. Price, Samant, S. S., Sigman, R. K., Meyer, W. L., Powell, E. A., Handley, J. C., and Strahle, W. C., “The Fire Environment of A Solid Rocket Propellant Burning In Air”, Air Force Weapons Laboratory, Kirtland Air Force Base, New Mexico 87117. AFWL Contract No. F29601-76-C-0119.

[9] Sigman, R. K., Dokhan, A., Price, E. W., Seitzman, J. M., and Lillard, R. P., “ Size Distribution Of Residual Oxide in Aluminized Propellants”, 37th JANNAF Combustion Meeting, Monterey, CA, November 2000

[10] Price, E. W., Chakravarthy, S. R., Sambamurthi, J. K., and Sigman, R. K., "The Details of Combustion of Ammonium Perchlorate Propellant: Leading Edge Flame Detachment," Combustion Science and Technology, 1998, Vol. 138, pp. 63-83.

[11] Sigman, R. K., Zachary, E. K., Chakravarthy, Freeman, J. M., and Price, E. W., “Preliminary Characterization of the Combustion Behavior of Alex in Solid Propellants”, Proceedings of the 34th JANNAF Combustion Meeting, Chemical Propulsion Information Agency.